# Extreme nonlinear response of ultranarrow optical transitions in cavity QED for laser stabilization

M. J. Martin,[1] D. Meiser,[1] J. W. Thomsen,[2] Jun Ye,[1] and M. J. Holland[1]

[1]*JILA, National Institute of Standards and Technology and Department of Physics,*
*The University of Colorado, Boulder, Colorado 80309-0440, USA*
[2]*The Niels Bohr Institute, Universitetsparken 5, DK-2100 Copenhagen, Denmark*

We explore the potential of direct spectroscopy of ultranarrow optical transitions of atoms localized in an optical cavity. In contrast to stabilization against a reference cavity, which is the approach currently used for the most highly stabilized lasers, stabilization against an atomic transition does not suffer from Brownian thermal noise. Spectroscopy of ultranarrow optical transitions in a cavity operates in a very highly saturated regime in which nonlinear effects such as bistability play an important role. From the universal behavior of the Jaynes-Cummings model with dissipation, we derive the fundamental limits for laser stabilization using direct spectroscopy of ultranarrow atomic lines. We find that, with current lattice clock experiments, laser linewidths of about 1 mHz can be achieved in principle, and the ultimate limitations of this technique are at the 1 $\mu$Hz level.

## I. INTRODUCTION

Ultrastable lasers are central components of optical atomic clocks and precision spectroscopy. Today's most stable lasers are made by locking the frequency of a prestabilized laser to a resonance of a high-finesse reference cavity [1–3]. The phase stability of these lasers is limited by thermal noise in the mirrors of the reference cavity [4]. They achieve linewidths below 1 Hz [5] corresponding to oscillator quality factors ($Q$ factors) of order $10^{15}$. Improvement of laser stability beyond the current state of the art will have a significant impact on precision science and quantum metrology [6], but further advances in laser stability through refinement of reference cavities require a significant investment in resources, given the maturity of the optical designs involved [7]. The purpose of this paper is to propose an alternative laser stabilization technique, by means of direct cavity-enhanced nonlinear spectroscopy and to elucidate the rich phenomenology of this approach in an extreme regime of cavity quantum electrodynamics and optical bistability.

Strong optical transitions typically used for laser stabilization are not suitable for ultimate laser stability since the atomic transition frequency is very sensitive to stray fields, collisions, etc. However, for special ultranarrow optical clock transitions that are now being routinely used for optical atomic clocks [8–10], these shifts are small, very well characterized, and can in some cases be eliminated or controlled [11].

Compared to the use of strong transitions, the physics of this frequency-locking scheme is nontrivial because the atomic transition is strongly saturated for very small intensities. Additionally, sufficient free-space optical depths are not available in current-generation experiments. One can circumvent this problem by working in a cavity-enhanced, highly non-linear, strongly saturated regime in order to achieve a signal that is strong enough for laser feedback. This regime has been studied extensively in the context of nonlinear optics with alkali-metal atoms [12–15], albeit in a much less extreme limit.

In this paper we consider a simplified model that contains all the essential components of this many-atom cavity QED system (Fig. 1), but in the extreme bad-cavity limit. Here, despite the unavoidable strong saturation effect, we are able to uncover a collective atomic interaction regime where we

preserve the superior frequency discrimination capability of a narrow atomic transition. This model serves as a basis upon which to calculate the fundamental limitations of our stabilization scheme, although real-world implementations will require more complicated topologies. One such approach could be based on the NICE-OHMS (noise-immune cavity-enhanced optical heterodyne molecular spectroscopy) technique [16,17], where the local oscillator and signal beams are copropagated through the cavity to reject common-mode frequency noise. The effects of finite vacuum lifetime and heating could be addressed by operating two systems in a multiplexed fashion, while heating could additionally be mitigated at the single-system level by implementing a Raman cooling scheme similar to that proposed in [18].

## II. MODEL SYSTEM

In our simplified theoretical analysis, we consider an ensemble of $N$ two-level atoms with transition frequency $\omega_a$ trapped in an optical lattice potential inside a cavity. The lattice is at the magic wavelength where the difference of the ac Stark shifts of both levels vanish [19]. The atoms are assumed to be in the vibrational ground state along the lattice direction and in the Lamb-Dicke regime such that we can neglect Doppler broadening and recoil effects. The atomic transition is near resonant with a cavity resonance with frequency $\omega_c$ and field decay rate $\kappa$. A laser with frequency $\omega_L$ is coupled into the cavity and the transmitted light is detected by means of balanced homodyne detection.

This $N$-atom system is described by the Hamiltonian

$$\hat{H} = \frac{\hbar\omega_a}{2}\sum_{j=1}^{N}\hat{\sigma}_z^{(j)} + \hbar\omega_c\hat{a}^\dagger\hat{a} + \hbar\eta(e^{-i\omega_L t}\hat{a}^\dagger + \text{H.c.})$$
$$+ \hbar g\sum_{j=1}^{N}(\hat{a}^\dagger\hat{\sigma}_-^{(j)} + \text{H.c.}). \qquad (1)$$

Here, $\hat{\sigma}_z^{(j)} = |e_j\rangle\langle e_j| - |g_j\rangle\langle g_j|$ is the operator for the inversion of atom $j$, and $\hat{\sigma}_+^{(j)} = |e_j\rangle\langle g_j|$ and $\hat{\sigma}_-^{(j)} = |g_j\rangle\langle e_j|$ are spin raising and lowering operators, respectively. The bosonic field operator $\hat{a}$ is the annihilation operator for a photon in the cavity.
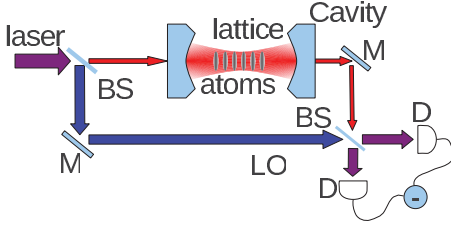
FIG. 1. (Color online) Schematic of cavity-enhanced ultranarrow-linewidth absorption spectroscopy for laser stabilization. M, mirror; BS, beam splitter; LO, local oscillator; D, photodiode.

The coupling constant $g = (\wp/\hbar) \sqrt{\hbar\omega_c/(2V_{\text{eff}}\epsilon_0)}$ is half the vacuum Rabi frequency with $V_{\text{eff}}$ the effective mode volume of the cavity, $\wp$ the dipole moment of the atomic transition, and $\epsilon_0$ the vacuum permittivity. The cavity is classically driven with amplitude $\eta$ by the in-coupled laser.

In addition to the coherent dynamics described by the Hamiltonian, we also need to account for dissipative processes. These are spontaneous emission from the excited atomic state (decay rate $\gamma$), decay of the atomic dipole with rate $T_2^{-1}$, and decay of the cavity field with rate $\kappa$. We treat these dissipative processes within the usual Born-Markov master equation [20]. Although we do not consider inhomogeneous atom-cavity coupling, this effect does not change our results qualitatively and can in principle be taken into account primarily by a rescaling of the cooperativity parameter via an effective atom number.

We assume that the cavity is locked to the probe laser, i.e., $\omega_L = \omega_c$. This could be achieved, for example, by using a frequency-offset Pound-Drever-Hall locking scheme [21] on a different cavity longitudinal mode in conjunction with a piezo-tunable cavity. Effects due to a slight detuning between laser and cavity are negligible owing to the comparatively large cavity linewidth, and we further quantify this statement in Appendix B.

### III. ANALYSIS

To study the nonlinear dynamics of this system, we consider a semiclassical approximation where all expectation values of more than one operator can be factorized, e.g., $\langle\hat{a}^{\dagger}\hat{\sigma}_-^{(j)}\rangle \approx \langle\hat{a}^{\dagger}\rangle\langle\hat{\sigma}_-^{(j)}\rangle$. Consequently, we find the set of first-order equations of motion for the expectation values $o \equiv \langle\hat{o}\rangle$ with $\hat{o} \in \{\hat{a}, \hat{\sigma}_-, \hat{\sigma}_z\}$,

$$\frac{da}{dt} = \eta - \kappa a + gN\sigma_-, \tag{2}$$

$$\frac{d\sigma_-}{dt} = -\left(T_2^{-1} + i\Delta\right)\sigma_- + ga\sigma_z, \tag{3}$$

$$\frac{d\sigma_z}{dt} = -\gamma(1 + \sigma_z) - 4g\text{Re}(a\sigma_-^*). \tag{4}$$

The atom-cavity detuning is $\Delta = \omega_a - \omega_c$.

The steady state of the system is obtained by setting the time derivatives to zero. The steady-state polarization of the atoms is given by

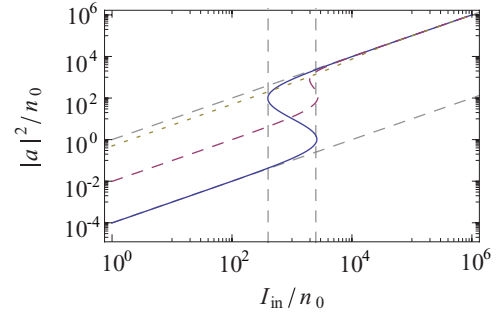$$\sigma_- = \frac{g}{T_2^{-1} + i\Delta} a\sigma_z. \tag{5}$$



FIG. 2. (Color online) Intracavity intensity as a function of in-coupled intensity for $\mathcal{C} = 100$ and $\Delta = 0$ (blue solid line), $\Delta = 10T_2^{-1}$ (purple dashed line), and $\Delta = 100T_2^{-1}$ (yellow dotted line). The vertical dashed lines mark the lower and upper thresholds for bistability. The diagonal dashed lines show the intracavity intensity for a completely bleached atomic ensemble, $|a|^2 = I_{\text{in}}$, and for the unsaturated limit, $|a|^2 = I_{\text{in}}/(2\mathcal{C})^2$. The saturation photon number is $n_0 = \gamma T_2^{-1}/(4g^2)$.

Inserting this into the equations for the inversion, we find the saturated inversion

$$\sigma_z = \frac{-1}{1 + \frac{|a|^2/n_0}{1 + T_2^2\Delta^2}}, \tag{6}$$

where $n_0 = \gamma T_2^{-1}/(4g^2)$ is the saturation photon number. The mean number of photons in the cavity is then

$$|a|^2 = \frac{\eta^2}{\kappa^2} \frac{1 + T_2^2\Delta^2}{(1 - \mathcal{C}\sigma_z)^2 + T_2^2\Delta^2}. \tag{7}$$

Here, $\mathcal{C} = N\mathcal{C}_0$ is the cooperativity parameter and $\mathcal{C}_0 = g^2/(\kappa T_2^{-1})$ is the single-atom cooperativity parameter.

In this proposal we consider a regime of high cooperativity where the total optical depth of the atom-cavity ensemble is greater than unity in the weak-driving limit. Specifically, in order to enter the nonlinear regime of spectroscopy considered here, the total cooperativity must satisfy $\mathcal{C} > 8$. The solution for the steady-state intensity with $\mathcal{C} = 100$ is illustrated in Fig. 2. For low in-coupled intensity, $I_{\text{in}} \equiv \eta^2/(n_0\kappa^2) < 4\mathcal{C}$, the atoms and cavity behave like two coupled harmonic oscillators. For $\omega_a = \omega_c$ the resonances of the coupled system are split by $2g\sqrt{N}$, the vacuum Rabi splitting. Hence, the driving field is far detuned from the coupled-system resonances for $\Delta = 0$, and the intensity inside the cavity is reduced by a factor $1/\mathcal{C}^2$ compared to an empty cavity. On the other hand, in the strong-driving limit, $I_{\text{in}} > \mathcal{C}^2/4$, the atomic transition is completely saturated, and the cavity behaves as if it were empty. In the intermediate regime, $4\mathcal{C} < I_{\text{in}} < \mathcal{C}^2/4$, two stable solutions exist; a low-intensity branch on which the atomic transition is unsaturated and a high-intensity branch on which it is saturated.

To clarify the connection of the physics considered here with previous studies of optical bistability in cavity QED, it is useful to consider the intensity in the cavity as a function of $\Delta$ and $\omega_c - \omega_L$. One of the stable solutions for the intracavity intensity is shown in Fig. 3. In the weak-driving limit, $I_{\text{in}} \to 0$, the resonances of the system approach the white hyperbolas while the resonance of the strongly driven system, $I_{\text{in}} \to \infty$, lies on the black horizontal line. Remarkably, with the axis
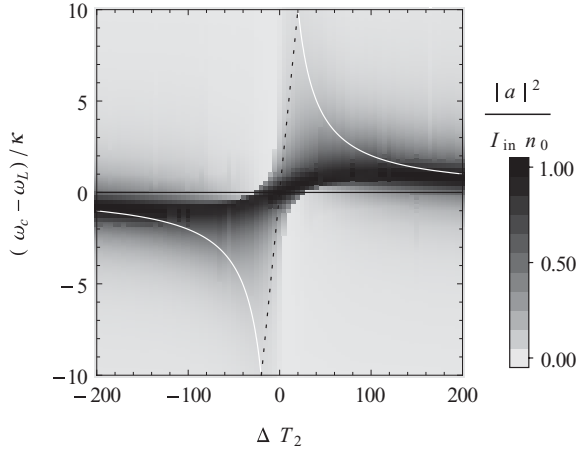
FIG. 3. Intracavity intensity as a function of detuning of the driving laser from the atomic resonance and from the cavity for $\mathcal{C} = 100$ and $I_{\mathrm{in}} = 5 \times 10^3$. Only the solution with the largest intracavity intensity is shown. Near resonance there are two additional solutions (see Fig. 4). The white hyperbolas indicate the resonances of the weakly driven system.

rescaled as in that figure, the plots depend only on two free parameters $C$ and $I_{\mathrm{in}}$. Most experiments on optical bistability in cavity QED to date have been carried out in a regime where $C/T_2 \gg \kappa$. For such an experiment, scanning $\omega_L$ with $\omega_a = \omega_c$ corresponds to the nearly vertical dotted line in this figure [13,22]. In our proposal $\Delta$ is scanned while $\omega_c = \omega_L$ at all times, corresponding to the black horizontal line. While the basic physics behind this nonlinear coupled system has been known for a long time [22], it has not been interrogated in the way discussed here.

The spectra resulting from scanning $\Delta$ in this way are shown for weak, intermediate (i.e., bistable), and strong pumping in Fig. 4. These spectra are cuts through the plot in Fig. 3 along the $\Delta = 0$ line. In the weak-pumping regime (dotted line), we see a broadened absorption feature with width $\mathcal{C}T_2^{-1}$. In the bistable regime (dashed line), there are three possible stationary values of the intracavity intensity near resonance. The solutions corresponding to largest and smallest intensity are dynamically stable while the intermediate-intensity solution is dynamically unstable. In the strong-pumping regime (solid line), there is
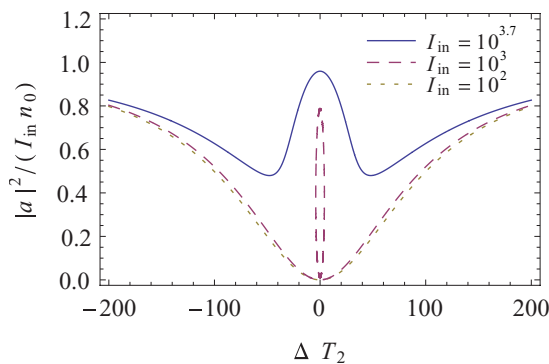


FIG. 4. (Color online) Intracavity intensity for $\mathcal{C} = 100$ as a function of detuning for in-coupled intensities $I_{\mathrm{in}} = 5 \times 10^3$ (blue solid line), $1 \times 10^3$ (purple dashed line), and $1 \times 10^2$ (yellow dotted line).

only one steady state for any detuning and a *peak* develops near resonance. Physically, this peak emerges because near resonance the atomic transition is strongly saturated, whereas away from resonance the cavity field experiences an additional phase shift due to the atoms and does not build up in the cavity.

## IV. APPLICATION TO LASER STABILIZATION

In this work, our idea is to lock the probe laser and cavity to this strongly saturated resonance feature. To estimate the potential performance of such a lock, we need to know the signal power and the slope of the phase across the resonance. The signal power is equal to the power leaking out of the cavity in steady state, and is given by

$$P \simeq \hbar\omega_L \kappa \mathcal{C}^2 n_0 \beta / 2 = 2\hbar\omega_L \eta^2 / \kappa, \qquad (8)$$

where the parameter $\beta = 4I_{\mathrm{in}}/(\mathcal{C}^2) \gtrsim 1$ describes how far above the upper threshold for bistability the system is driven. This power corresponds to a photon shot-noise-limited bandwidth-normalized signal-to-noise ratio of $\mathcal{R}_{S/N}^2 = \kappa \mathcal{C}^2 n_0 \beta$ (Hz), assuming unity photodetector quantum efficiency. Specifically, near resonance, we can write the differential photocurrent from the system as

$$i_{\mathrm{diff}} = \frac{2e}{h\nu}\sqrt{P_{\mathrm{sig}}P_{\mathrm{LO}}}\frac{d\phi}{d\nu}\delta\nu(t) + \delta i(t). \qquad (9)$$

Here, $\phi$ is the frequency-dependent phase shift imparted by the intracavity atomic medium near atomic resonance, $\delta i(t)$ is the shot noise on the photodetector difference signal, $\delta\nu(t)$ is the system detuning from exact atomic resonance, and $P_{\mathrm{LO(sig)}}$ is the optical power in the LO (signal) pathway. Shot noise will contaminate the resonance condition as

$$\delta\nu(t) = -\delta i(t)\frac{h\nu}{2e\sqrt{P_{\mathrm{sig}}P_{\mathrm{LO}}}\frac{d\phi}{d\nu}}. \qquad (10)$$

The phase shift near atomic resonance is linear to first order for small frequency deviations, and is given by

$$\frac{d\phi}{d\Delta} = T_2\frac{\mathcal{C}\sigma_z}{\mathcal{C}\sigma_z - 1} = \frac{4T_2}{\beta\mathcal{C}} + O(\mathcal{C}^{-2}). \qquad (11)$$

The shot-noise-limited photocurrent noise has a white power spectrum and, in the limit of $P_{\mathrm{LO}} \gg P_{\mathrm{sig}}$, the magnitude is proportional to $\frac{e^2}{h\nu}P_{\mathrm{LO}}$. As a consequence, the frequency noise power spectral density of the lock error, $S_{\delta\nu}$, is white. We convert this quantity to a conventional laser linewidth (see, e.g., [24,25] and Appendix A) when the system is locked and find that

$$\Delta\nu = 2\pi S_{\delta\nu} = \pi\left(\frac{1}{\mathcal{R}_{S/N}2\pi\frac{d\phi}{d\Delta}}\right)^2 \approx \frac{\mathcal{C}_0}{16\pi\gamma T_2^2}\beta. \qquad (12)$$

This is the key result of this paper, as it represents the quantum-limited linewidth $\Delta\nu$ of a laser stabilized to the nonlinear resonance feature discussed in this work.

It is worth contrasting these results with the ones obtained for a proposed active laser based on ultranarrow optical transitions [18]. For that system the linewidth is given by

TABLE I. Quantum-limited linewidth according to Eq. (A19) for several optical lattice clock systems. The cavity geometry is $V_{\text{eff}} = L \times (100 \ \mu\text{m})^2$ and the finesse $\mathcal{F}$ is tuned to give $N\mathcal{C}_0 \simeq 100$. The signal-to-noise ratio (SNR) is 1 Hz bandwidth normalized. In all but the last case, $T_2$ values have been set to be $\leqslant 1$ s. This is a conservative estimate based on current-generation lattice clock experiments [23].

| Transition | $\lambda$ | $T_2^{-1}$ | $\gamma$ | $N$ | $\mathcal{F}$ | $\mathcal{C}_0$ | $P(\beta = 2)$ | SNR | $\Delta\nu$ |
|---|---|---|---|---|---|---|---|---|---|
| $^{24}\text{Mg}^1S_0 \to {}^3P_1$ | 457 nm | $\gamma/2$ | $2\pi \times 31$ Hz | $10^4$ | $10^4$ | $9.6 \times 10^{-3}$ | 20 pW | $9.8 \times 10^3$ | 20 mHz |
| $^{87}\text{Sr}^1S_0 \to {}^3P_0$ | 698 nm | $1\ \text{s}^{-1}$ | $2\pi \times 1$ mHz | $10^5$ | $10^5$ | $7.4 \times 10^{-4}$ | 3 fW | $1.5 \times 10^2$ | 4.7 mHz |
| $^{171}\text{Yb}^1S_0 \to {}^3P_0$ | 578 nm | $1\ \text{s}^{-1}$ | $2\pi \times 44$ mHz | $10^4$ | $5 \times 10^4$ | $1.1 \times 10^{-2}$ | 27 fW | $3.9 \times 10^2$ | 1.6 mHz |
| $^{199}\text{Hg}^1S_0 \to {}^3P_0$ | 265.6 nm | $1\ \text{s}^{-1}$ | $2\pi \times 100$ mHz | $10^4$ | $10^5$ | $1.1 \times 10^{-2}$ | 130 fW | $5.8 \times 10^2$ | 0.68 mHz |
| $^{87}\text{Sr}^1S_0 \to {}^3P_0$ | 698 nm | $\gamma/2$ | $2\pi \times 1$ mHz | $10^4$ | $5 \times 10^3$ | $1.2 \times 10^{-2}$ | 0.5 fW | $6.1 \times 10^1$ | 0.74 $\mu$Hz |

$\Delta\nu_{\text{laser}} = \mathcal{C}_0 \gamma / \pi$. The atoms behave more collectively in the case of the laser. At the peak of laser emission the collective dipole of the atoms is proportional to $N$, i.e., $\langle \hat{J}_+ \hat{J}_- \rangle \propto N^2$, where $\hat{J}_- = \hat{J}_+^\dagger = \sum_{j=1}^N \hat{\sigma}_-$. In contrast, for the passive spectroscopy considered here,

$$\langle \hat{J}_+ \hat{J}_- \rangle = \frac{N^2}{\mathcal{C}^2} \frac{T_2 \gamma}{\beta} \qquad (13)$$

on resonance, $\Delta = 0$, i.e., the effective number of atoms that participate in the collective dynamics is reduced by a factor of order $\sqrt{T_2 \gamma}$. Finally, we note that in the limit where there is no inhomogeneous broadening ($T_2 = 2/\gamma$), Eq. (A19) reduces to $\Delta\nu = \beta \mathcal{C}_0 \gamma / (64\pi)$. This is, for $\beta$ of order unity, the same scaling as in the laser case.

Table I summarizes the stabilization performance that can be achieved for several atomic species and transitions. In all these examples the parameters are chosen such that $\mathcal{C} \approx 100$. The mode volume of the cavity is $V_{\text{eff}} = L \times \pi (100 \ \mu\text{m})^2$, where the length $L$ does not enter the results. Furthermore, in this locking scheme, the quantum-limited lock bandwidth (beyond which the signal-to-noise ratio drops below unity) is given by $\mathcal{B}_{\text{ql}} = \kappa \mathcal{C}^2 n_0 \beta$. In all cases considered, this fundamental limitation is well above the kilohertz range, indicating that the requisite level of laser prestabilization is well within current technological capabilities. In several realistic lattice clock systems, we find that laser stabilization can achieve quantum-limited performance at the millihertz level without suffering from thermal noise. Finally, improvements in the coherence time $T_2$ of the narrowest transitions yield reciprocal gains in the quantum-limited locked-laser linewidth, underscoring the importance of investigating possible decoherence mechanisms for neutral atom lattice clocks beyond the 1 s time scale.

## V. CONCLUSION

We have proposed a laser stabilization technique based on strongly saturated spectroscopy of narrow optical transitions that enables linewidths in the 1 mHz range with current experimental technology. This technique is not limited by thermal noise and the fundamental limits of this scheme are below the $1 \mu$Hz level. In the future we plan to study alternative realizations of this idea, including atomic beams and trapped ions.

## APPENDIX A: DERIVATION OF LOCKED LASER LINEWIDTH

In this Appendix we derive in detail the expression for the quantum-noise-limited linewidth, which is presented in Eq. (12). We begin by considering the configuration shown in Fig. 1. The photocurrents of detectors 1 and 2 are given by

$$i_{1,2} = \frac{e\eta_{\text{qe}}}{h\nu} \left[ \frac{P_{\text{sig}}}{2} + \frac{P_{\text{LO}}}{2} \pm \sqrt{P_{\text{sig}} P_{\text{LO}}} \cos(\Delta\varphi - \phi_{\text{LO}}) \right] + \delta i_{1,2}(t), \qquad (A1)$$

with the "+" ("−") corresponding to detector 1 (2). Here, $\Delta\varphi$ is the additional phase shift acquired by the signal beam, $P_{\text{LO}}$ is the power in the local oscillator pathway, $P_{\text{sig}}$ is the power in the signal pathway, $\eta_{\text{qe}}$ is the detector quantum efficiency, and $\delta i_{1,(2)}$ is the stochastically fluctuating component of the photocurrent at detector 1 (2) due to shot noise. Thus, with the proper choice of LO phase and assuming $\Delta\varphi \ll 1$,

$$i_{\text{diff}}(t) = i_1 - i_2 = \frac{2e\eta_{\text{qe}}}{h\nu} \sqrt{P_{\text{sig}} P_{\text{LO}}} \Delta\varphi + \delta i_1(t) - \delta i_2(t). \qquad (A2)$$

We rewrite the term $\delta i_1(t) - \delta i_2(t)$ as $\delta i(t) \equiv \delta i_1(t) - \delta i_2(t)$. The time-domain autocorrelation of $\delta i(t)$ is given by

$$\langle \delta i(t) \delta i(t + \tau) \rangle = \frac{e^2 \eta_{\text{qe}}}{h\nu} [P_{\text{sig}} + P_{\text{LO}}] \delta(\tau)$$

$$\simeq \frac{e^2 \eta_{\text{qe}}}{h\nu} P_{\text{LO}} \delta(\tau). \qquad (A3)$$

Here, $\delta(\tau)$ is the Dirac delta function. This corresponds to a two-sided photocurrent noise power spectral density of

$$S_i(f) = \frac{e^2 \eta_{\text{qe}}}{h\nu} P_{\text{LO}}. \qquad (A4)$$

The resonance center is observed in this system via the difference photocurrent—namely, where the difference photocurrent is equal to zero. In order to see the effect of
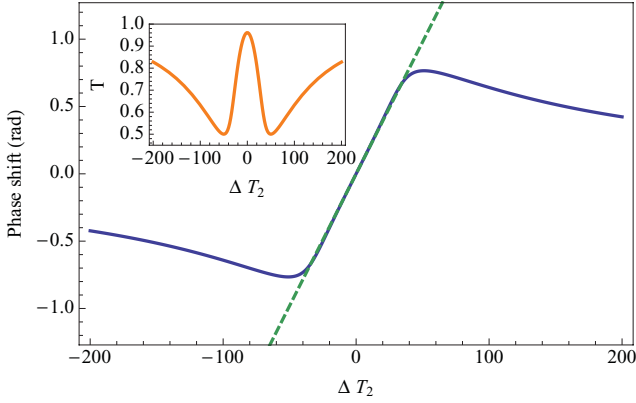
FIG. 5. (Color online) Phase shift of the transmitted cavity light (with respect to the LO) due to the atomic medium inside the cavity and as a function of laser detuning. Here, $\mathcal{C} = 100$ and $\beta = 2$. The dotted line is the linear approximation for the phase near zero detuning. Inset: Cavity transmission curve for the same parameters.

the LO shot noise on the lock stability, one can expand $i_{\text{diff}}$ about zero detuning to linear order of $\Delta\nu$ as

$$i_{\text{diff}} = \frac{2e\eta_{\text{qe}}}{h\nu}\sqrt{P_{\text{sig}}P_{\text{LO}}}\,\Delta\varphi + \delta i\,(t)$$

$$\simeq \frac{2e\eta_{\text{qe}}}{h\nu}\sqrt{P_{\text{sig}}P_{\text{LO}}}\,\frac{\partial\varphi}{\partial\nu}\Delta\nu + \delta i\,(t). \quad \text{(A5)}$$

The validity of making this linear approximation is shown in Fig. 5, where the complete phase shift of the medium is shown as a function of detuning from resonance along with an analytical solution for the linear phase shift $\frac{\partial\varphi}{\partial\nu}\Delta\nu$. As long as the laser is close to resonance, the phase is linear to a good approximation. Now we can identify the effect of $\delta i(t)$ on our ability to determine the line center of the atomic resonance.

Under the locked condition, the DC difference current $I_{\text{diff}}$ is enforced to be zero via control of the laser frequency. We can thus see that the term $\delta i(t)$ corrupts the measurement. That is, our frequency error is given by

$$\Delta\nu_{\text{err}}\,(t) = \frac{\delta i\,(t)}{\frac{2e\eta_{\text{qe}}}{h\nu}\sqrt{P_{\text{sig}}P_{\text{LO}}}\frac{\partial\varphi}{\partial\nu}}. \quad \text{(A6)}$$

The denominator came directly from Eq. (A5).

When locked to the cavity-atom resonance, we assume the laser has an electric field given by

$$E(t) = E_0 e^{i2\pi\nu_0 t + i\delta\phi(t)}. \quad \text{(A7)}$$

Here the phase error $\delta\phi(t)$ is related to $\Delta\nu_{\text{err}}\,(t)$ by

$$\frac{d\delta\phi}{dt} \equiv \Delta\nu_{\text{err}}\,(t). \quad \text{(A8)}$$

In order to go from this time-domain expression to the frequency domain via the Wiener-Khinchin theorem (following the general approach presented in Chap. 3 of [26]), we compute the autocorrelation of the field amplitude, $R_E\,(\tau)$, given by

$$R_E\,(\tau) = \langle E(t)E^*(t+\tau)\rangle$$

$$= |E_0|^2 e^{i2\pi\nu_0\tau}\langle e^{i(\delta\phi(t)-\delta\phi(t+\tau))}\rangle. \quad \text{(A9)}$$

An application of the Gaussian moment theorem gives

$$\langle e^{i[\delta\phi(t)-\delta\phi(t+\tau)]}\rangle = \exp\{-\langle[\delta\phi(t)-\delta\phi(t+\tau)]^2\rangle/2\}. \quad \text{(A10)}$$

We can rewrite the expectation value as

$$\langle[\delta\phi(t)-\delta\phi(t+t)]^2\rangle = 2\langle[\delta\phi(t)]^2\rangle - 2\langle[\delta\phi(t)\delta\phi(t+\tau)]\rangle$$

$$= 2[R_\phi(0) - R_\phi(\tau)]. \quad \text{(A11)}$$

It is then a direct consequence of the Wiener-Khinchin theorem that

$$\langle[\delta\phi(t)-\delta\phi(t+\tau)]^2\rangle = 2\left[\int_{-\infty}^{\infty} S_{\delta\phi}(f)(1-e^{i2\pi f\tau})df\right], \quad \text{(A12)}$$

where $S_{\delta\phi}\,(f)$ is the two-sided phase fluctuation power spectral density for $\delta\phi(t)$. However, we can easily relate $S_{\delta\phi}$ to $S_{\Delta\nu}$ (the two-sided frequency deviation power spectral density) by Eq. (A8), such that

$$\langle[\delta\phi(t)-\delta\phi(t+\tau)]^2\rangle = 2\left[\int_{-\infty}^{\infty} \frac{S_{\Delta\nu_{\text{err}}}(f)}{f^2}(1-e^{i2\pi f\tau})df\right]. \quad \text{(A13)}$$

Applying the Wiener-Khinchin theorem to Eq. (A6), we have

$$S_{\Delta\nu_{\text{err}}} = \frac{h\nu}{4\eta_{\text{qe}}P_{\text{sig}}\left(\frac{\partial\varphi}{\partial\nu}\right)^2}. \quad \text{(A14)}$$

We can therefore rewrite Eq. (A13) as

$$\langle[\delta\phi(t)-\delta\phi(t+\tau)]^2\rangle = \int_0^{\infty} \frac{b_0}{f^2}\left[1-\cos\left(2\pi f\tau\right)\right]df$$

$$= b_0\pi^2\tau, \quad \text{(A15)}$$

with $b_0$ given by

$$b_0 = \frac{h\nu}{\eta_{\text{qe}}P_{\text{sig}}\left(\frac{\partial\varphi}{\partial\nu}\right)^2}. \quad \text{(A16)}$$

Now we have an expression for the electric field autocorrelation, namely,

$$R_E(\tau) = |E_0|^2 e^{i2\pi\nu_0\tau}e^{-b_0\pi^2\tau/2}. \quad \text{(A17)}$$

We apply the Wiener-Khinchin theorem to this expression and obtain a Lorentzian profile for the laser optical power, with frequency full width at half maximum, $\Delta\nu_{\text{FWHM}}$, given by

$$\Delta\nu_{\text{FWHM}} = \frac{\pi b_0}{2} = \frac{\pi h\nu}{2\eta_{\text{qe}}P_{\text{sig}}\left(\frac{\partial\varphi}{\partial\nu}\right)^2}. \quad \text{(A18)}$$

We combine this with the results of Eqs. (8) and (11) of the main text, and obtain the result presented in Eq. (12), in the limit of unity detector quantum efficiency, namely,

$$\Delta\nu \approx \frac{\mathcal{C}_0}{16\pi\gamma T_2^2}\beta. \quad \text{(A19)}$$

## APPENDIX B: LINE-PULLING EFFECTS DUE TO CAVITY-LASER DETUNING

In order to derive the line pulling due to an imperfect lock between the cavity and probe laser, we make use of the

full optical bistability equation that describes the input-output steady state of the system [27],

$$y = x \left( 1 + \mathcal{C} \frac{1 - iT_2\Delta}{1 + |x|^2 + (T_2\Delta)^2} + i\theta \right). \quad \text{(B1)}$$

The parameter $x$ is related to $\langle a \rangle$ by $x = \langle a \rangle / \sqrt{n_0}$, $y$ is given by $\eta/(\kappa\sqrt{n_0})$ ($|y|^2 = I_{in}$), $\Delta$ and $T_2$ are the same as given in the text, and the parameter $\theta$ is the cavity-laser detuning in units of $\kappa$, namely, $\theta = (\omega_c - \omega_l)/\kappa$. In the text, $\theta$ was assumed to be negligibly small. Here we quantify this statement.

If we assume that we are near resonance in the nonlinear, strongly saturated regime ($\beta > 1$, $\mathcal{C} \gg 1$), then $|y|^2 \simeq |x|^2 = \beta\mathcal{C}^2/4$. If $T_2\Delta \ll \mathcal{C}$, then we can expand Eq. (B1) such that

$$y \simeq x \left[ 1 + \frac{4}{\mathcal{C}\beta} (1 - iT_2\Delta) + i\theta \right]. \quad \text{(B2)}$$

Therefore, the phase shift of the transmitted light is given by

$$\Delta\phi = \text{Arg}\,[x/y] \simeq \frac{4T_2\Delta}{\mathcal{C}\beta} - \theta. \quad \text{(B3)}$$

From Eq. (B3), it can be seen that for a given cavity-laser detuning, the lock-center frequency shift $\Delta\nu_{laser}$ is given by

$$\Delta\nu_{laser} = \frac{\mathcal{C}\beta}{8\pi T_2} \left( \frac{\omega_c - \omega_l}{\kappa} \right). \quad \text{(B4)}$$

Cavity lock precisions of $> 10^4$ are routinely achieved in the laboratory. This implies that

$$\left( \frac{\omega_c - \omega_l}{\kappa} \right) \lesssim 10^{-4}. \quad \text{(B5)}$$

For typical parameters considered in the main text, namely, $\mathcal{C} = 100$, $\beta = 2$, and $T_2 = 1$ s, this implies that the cavity pulling effect is below the 1 mHz level. Longer $T_2$ times will further suppress this effect.

---

[1] R. W. P. Drever *et al.*, Appl. Phys. B **31**, 97 (1983).

[2] B. C. Young, F. C. Cruz, W. M. Itano, and J. C. Bergquist, Phys. Rev. Lett. **82**, 3799 (1999).

[3] Y. Y. Jiang *et al.*, Nat. Photon. **5**, 158 (2011).

[4] K. Numata, A. Kemery, and J. Camp, Phys. Rev. Lett. **93**, 250602 (2004).

[5] A. Ludlow *et al.*, Opt. Lett. **32**, 641 (2007).

[6] S. Diddams, J. Bergquist, S. Jefferts, and C. Oates, Science **306**, 1318 (2004).

[7] L. Chen, J. L. Hall, J. Ye, T. Yang, E. Zang, and T. Li, Phys. Rev. A **74**, 053801 (2006).

[8] T. Rosenband *et al.*, Science **319**, 1808 (2008).

[9] A. D. Ludlow *et al.*, Science **319**, 1805 (2008).

[10] N. D. Lemke, A. D. Ludlow, Z. W. Barber, T. M. Fortier, S. A. Diddams, Y. Jiang, S. R. Jefferts, T. P. Heavner, T. E. Parker, and C. W. Oates, Phys. Rev. Lett. **103**, 063001 (2009).

[11] M. D. Swallows *et al.*, IEEE Trans. Ultrason. Ferroelectr. Freq. Control **57**, 574 (2010); Science **331**, 1043 (2011).

[12] P. D. Drummond, IEEE J. Quantum Electron. **QE-17**, 301 (1981).

[13] J. Gripp, S. L. Mielke, L. A. Orozco, and H. J. Carmichael, Phys. Rev. A **54**, R3746 (1996).

[14] S. L. Mielke, G. T. Foster, J. Gripp, and L. A. Orozco, Opt. Lett. **22**, 325 (1997).

[15] G. T. Foster, S. L. Mielke, and L. A. Orozco, Phys. Rev. A **61**, 053821 (2000).

[16] J. Ye, L.-S. Ma, and J. Hall, J. Opt. Soc. Am. B **15**, 6 (1998).

[17] A. Foltynowicz, F. Schmidt, W. Ma, and O. Axner, Appl. Phys. B **92**, 313 (2008).

[18] D. Meiser, J. Ye, D. R. Carlson, and M. J. Holland, Phys. Rev. Lett. **102**, 163601 (2009).

[19] J. Ye, H. Kimble, and H. Katori, Science **320**, 1734 (2008).

[20] D. Walls and G. Milburn, *Quantum Optics* (Springer-Verlag, Berlin, 2008).

[21] R. W. P. Drever *et al.*, Appl. Phys. B **31**, 97 (1983).

[22] J. Gripp, S. L. Mielke, and L. A. Orozco, Phys. Rev. A **56**, 3262 (1997).

[23] M. Boyd *et al.*, Science **314**, 1430 (2006).

[24] D. S. Elliott, R. Roy, and S. J. Smith, Phys. Rev. A **26**, 12 (1982).

[25] G. M. Stéphan, T. T. Tam, S. Blin, P. Besnard, and M. Têtu, Phys. Rev. A **71**, 043809 (2005).

[26] F. Riehle, *Frequency Standards Basics and Applications* (Wiley-VCH, Weinheim, Ger., 2004).

[27] J. Gripp, S. L. Mielke, and L. A. Orozco, Phys. Rev. A **56**, 3262 (1997).